

# ANALYSIS ON FLOW SEPARATION CHARACTERISTICS OF LAST STAGE BLADE IN STEAM TURBINE UNDER SMALL VOLUME FLOW CONDITION

Lihua CAO<sup>a\*</sup>, Wenlong WANG<sup>a</sup>, Huanhuan LUO<sup>b</sup>, Pengfei HU<sup>a</sup>, Zhengwen LI<sup>b</sup>, Yanjun ZHANG<sup>b</sup>, Dingshan MA<sup>c</sup>

<sup>a</sup> School of Energy and Power Engineering, Northeast Electric Power University, Jilin 132012, China

<sup>b</sup> State Grid Liaoning Electric Power Supply Co., Ltd. Liaoning 110004, China

<sup>c</sup> XI'AN Thermal Power Research Institute Co., Ltd. Xian 710054, China

\* Corresponding author: Lihua CAO<sup>a\*</sup>; E-mail:clh320@126.com

*The inlet steam flow of steam turbine is obviously reduced and even in the state of small volume flow when the thermal power unit is involved in peak load operation, which greatly influences the safety of steam turbine. The last stage flow field of steam turbine under small volume flow condition is calculated by the CFX to study the formation, development, influencing range and the variation rule of the flow separation vortex cores. The results show that the flow separation vortices appear near last stage blade at 30% of the rated volume flow. With the decrease of volume flow, the flow separation vortices gradually spread to the root of blade. When the volume flow decreases to 8% of the rated volume flow, the flow separation vortices almost occupy the whole blade. The position of the flow separation vortex cores shifts from 72.7% of the relative blade height to 49.1%. The results of this paper lay a foundation for the safety analysis of the last stage blade in the steam turbine under the small volume flow condition.*

*Key words: steam turbine; last stage blade; small volume flow; flow angle; flow separation vortices*

## 1. Introduction

With the rapid development of social economy and the increasing demand for energy, wind energy, solar energy and other clean energy are paid more attention in the power generation industry. In order to consume more new energy, the traditional coal-fired power plant with a peak load operation is the main solution. However, the flow field, especially in the last stage blade of low-pressure cylinder is very complicated when the steam turbine is under the low load or high backpressure conditions. The reaction degree in the root of the rotor blade declines due to the decreasing of volume flow. The flow will separate and reverse from the last stage blade because of the effect of the diffuser of stator blades and the centrifugal force of rotor blades [1]. A large range of separation vortices is formed on the pressure surface, which causes a dramatic change of the blades dynamic stress [2-4], as well as blades vibration [5-8]. When the volume flow decreases to a certain extent, the last stage blades will go into the steam blast condition, which leads to a sudden temperature increase and the over-temperature deformation of the blade surface [9]. Therefore, it is necessary to study the flow

characteristics of the last stage blades under the small volume flow conditions to improve the efficiency of the unit and ensure the safety of the last stage blade.

In recent years, a large number of scholars have conducted in-depth studies on the flow characteristics of the last stage blades under small volume flow condition[10-11]. Lei Qi et al. [1] simulated the steam flow of the last two stage blades under a low load condition and put forward the law that the height of flow separation varies with the volume flow. Xiaocheng Zhu et al. [12] pointed out that the last stage was in the blast condition when the backpressure is 55kPa. With the increase of backpressure, the last stage blades are heated by the friction and windage, which causes the over-temperature deformation of the last stage blades. Xiaoshu Cai et al. [13-14] studied the steam flow of last stage blades through experiment. It was pointed out that the blast state occupied over 50% of the whole blade height at 100% of the rated volume flow under high back pressure condition. M Benjamin[15], R Sigget al. [16] combined experiment with numerical simulation to study the steam flow of the last stage blade in small volume flow. It was shown that the test results were in good agreement with simulation. Under the very low flow conditions, the steam flow consumed a lot of energy to flow through the blades because the last stage blades were in the blast condition. However, the above research only explained the variation of steam temperature, pressure and other parameters in peak load conditions, the rules of flow separation vortices and the changes of vortex cores position caused by those parameters variation were not given.

In the study of the influence of small volume flow, B. Adam et al. [9] thought the vortex generated at the tip clearance between the stator and rotor blades with the decrease of volume flow was the main reason for surface temperature rise of the blade. S. Naoki [17-18] investigated the exciting force caused by small volume flow and pointed that it was related to the total mass flow, the smaller mass flow is, the greater exciting force is. S. Senoo et al. [19] pointed out the flow separation area under small volume flow condition. The above scholars mainly studied the over-temperature deformation and exciting force caused by small volume flow condition but the problem that the flow separation vortices spread to the stator blades and further deteriorate flow field with the reduce of volume flow were ignored.

I. Bosdas et al. [20-21] researched the pressure fluctuations on the suction and pressure surface at small volume flow conditions, but the flow field deterioration caused by the flow separation vortices was not considered. As the volume flow decreases, the deterioration intensifies and the flow separation vortices have a tendency of spreading to the stator blades. Besides, the pressure fluctuation caused by the flow separation vortices was not considered as well. In order to study the vortices migration with the decrease of volume flow, K. Segawa et al [22] set up monitoring points at the position of flow separation vortex cores in small volume flow. The above analyses only reflected the axial translation of the flow separation vortices but the radial expansion was not considered. The influencing range of the vortices was not clearly pointed out, either.

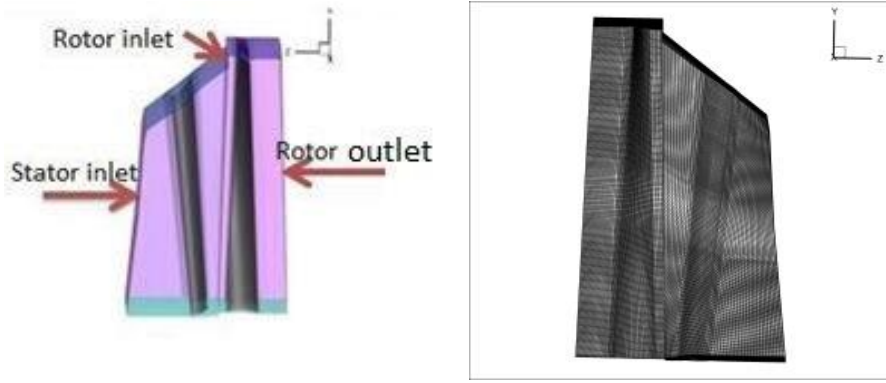
In summary, the steam flow in the last stage blade is very complex under the small volume flow condition. Large separation flow occurs in the last stage blade with the decrease of the volume flow, the shape of the separation flow on the blade surface changes with the further decrease of the volume flow. When the volume flow decreases to a certain extent, the blast condition will occur. It causes over-temperature deformation of the blades and seriously influences the safety and stable operation of steam turbine. Therefore, the primary objective of the paper is to study the formation, development, influencing range and the variation rule of the flow separation vortex cores under the small volume

flow conditions. Results presented here would aid to ensure the safety of the last blade.

## 2. Models and calculation methods

### 2.1 Model and boundary conditions

A physical model of the last stage in a 300MW steam turbine is studied. The number of rotor blades and stator blades are 80 and 52 respectively. As the number of rotor and stator blades is different, the mass flow through a stator blade flow passage is different from that through a rotor blade passage. To make the results more accurate and reduce computation amount, the physical model of 3 rotor blades and 2 stator blades is used. The physical model and grid of the last stage blades are shown in Fig.1.



(a) Physical model

(b) grid

Fig.1. Physical model and grid of last stage blade

The inlet total temperature, the inlet mass flow and the outlet static pressure are 336.15K, 3.33478kg/s and 4.9kPa respectively. The periodic boundary condition is used. The adiabatic and non-slip boundary conditions are applied on the stator blade surface. The rotating surface on the rotor blade is established and the rotating speed is 3000r/min. The frozen rotor model produces a steady state solution to the multiple frame of reference problems and takes some account of the interaction between the two frames. Therefore, it is applied at the interface between stator and rotor in this simulation.

### 2.2 Numerical methods and turbulence models

To simulate the compressible viscous flow in the last stage of steam turbine, the time-averaging continuity equation, Navier-Stokes equation and energy equation are solved by the finite volume method. The working medium in the last stage is wet steam which status parameters are provided by the IAPWS-IF97. Equilibrium phase change model is used to simulate the wet steam-droplet flow. The wet steam dryness is shown in Eq.(1):

$$\alpha = \frac{h - h_{\text{sat},f}(p)}{h_{\text{sat},g}(p) - h_{\text{sat},f}(p)} \quad (1)$$

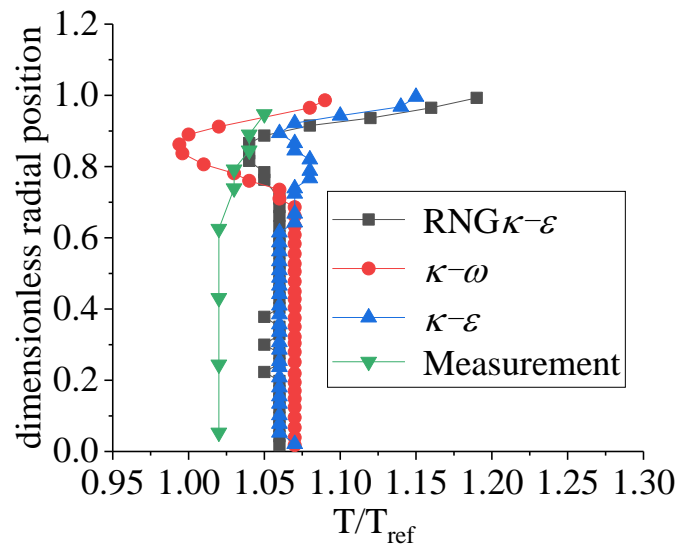
Where  $\alpha$  is the wet steam dryness,  $h_{\text{sat},f}(p)$  is the saturated water enthalpy,  $h_{\text{sat},g}(p)$  is the saturated steam enthalpy. When  $\alpha$  is between 0 and 1, The working medium turns to wet steam. The thermophysical parameters are determined by Eq.(2):

$$\varphi_{\text{mix}}(p) = (1 - \alpha) \varphi_{\text{sat},f}(p) + \alpha \varphi_{\text{sat},g}(p) \quad (2)$$

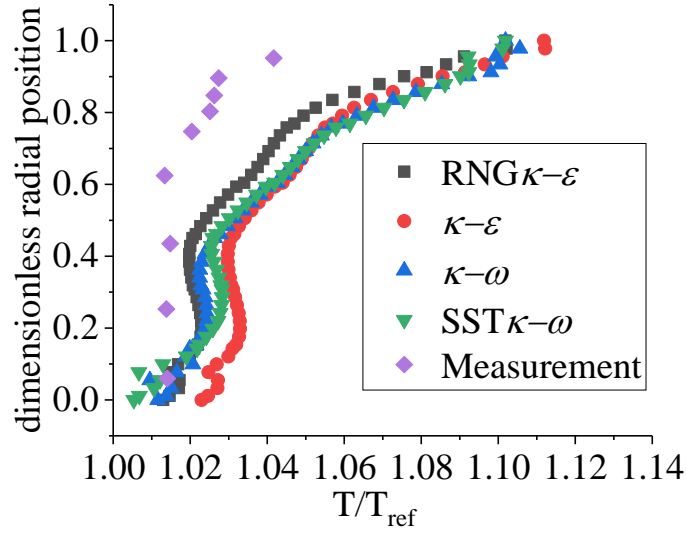
Where  $\varphi_{\text{mix}}(p)$  is the wet steam thermophysical parameters,  $\varphi_{\text{sat},f}(p)$  is the saturated water thermophysical parameter,  $\varphi_{\text{sat},g}(p)$  is the saturated gas parameter.

The steam separation is studied but the slip between steam and droplets and the influence of droplets on flow separation are not considered in this paper.

Scalable wall-function method and the boundary layer mesh refinement technology are used to simulate the flow. To obtain well boundary layer, the dimensionless distance from wall ( $y^+$ ) is ensured below 15 as the turbulence model requirement [23]. The difference scheme is the second order upwind solution mode and the limit value of convergence residuals is set to  $10^{-4}$ .



(a) The last four stage blades



(b)The last stage blade

Fig.2. Independence verification of turbulence model

The temperature ratio of the last four stage blades in the low pressure cylinder was measured under 10% of the rated volume flow condition and compared with the result by simulation in reference [9]. The RNG  $\kappa-\varepsilon$  turbulence model is relatively closest to the measured value as shown in Fig. 2(a). Different turbulence models are provided to study the temperature ratio of the last stage blade in steam turbine under the condition of reference[9] as shown in Fig. 2(b). The differences in temperature ratio are found between measurement and simulation in Fig 2. The reason of differences is that the inlet temperature of the last four stage blades is selected as reference temperatures in measurement, but the inlet temperature of the last stage blade is selected in simulation. Obviously, the inlet temperature in the last four stage blades is higher than that in the last stage blade. The temperature ratio in simulation is higher than that in measurement. The RNG  $\kappa-\varepsilon$  turbulence model in this paper is also relatively closest to the measured value as shown in Fig. 2(b). Therefore, the RNG $\kappa-\varepsilon$  turbulence model is selected in this paper.

### 2.3 Grid generation and independence

Rotor and stator blades meshes are generated by ANSYS TurboGrid and the "HOH" topology is used. In order to determine the optional grid number, validation of grid independence is carried out. Fig.3 illustrates the effects of grid number on the CFD results. The isentropic efficiency(Eq.(3)) is taken as reference parameters and it is found that the total grid number has little effect on the isentropic efficiency when the total grid number reaches to 3.5 millions. To reduce computation time, the total grid number of the flow passages is determined as 3.66 millions, in which the grid number of single rotor and stator blade is 0.74 millions and 0.72millions respectively.

$$\eta = (h_2 - h_1^*) / (h_2^{is} - h_1) \quad (3)$$

Where  $h_2$  and  $h_2^{is}$  is the average enthalpy and the average entropic enthalpy at the rotor outlet,

respectively.  $h_1^*$  and  $h_1$  is the average total enthalpy and the average enthalpy at the stator inlet, respectively.

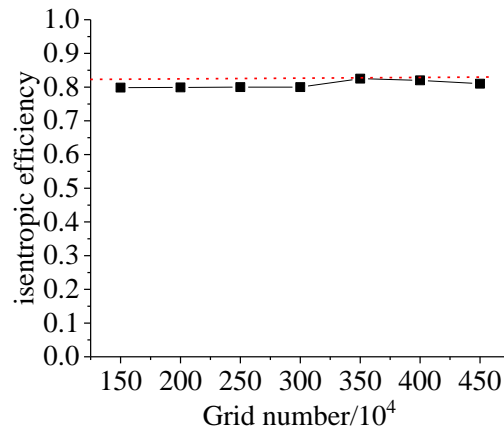


Fig.3 Grid independence verification

### 3. Results and analysis

#### 3.1 Flow angle

The flow angle of rotor outlet has an impact on the formation, development, influencing range and the variation rule of the flow separation vortex cores. Therefore, it is a key to reasonably determine the flow angle of rotor outlet under different volume flow conditions for studying the flow separation characteristics of the last stage blade. Speed triangle schematic diagram in rotor outlet is shown in Fig.4 where  $\beta_2$  is the flow angle of rotor outlet. Flow angles of rotor outlet shown in Fig. 5 are average values along the blade height. Because the steam parameters vary greatly along the blade height in the last stage blade, the steam parameters at the average diameter cannot be used to describe the flow state of the whole blade, ten planes are equally spaced along the blade height to calculate the speed triangle respectively. It can be seen from Fig. 5, the value of rotor outlet flow angle has a good agreement between the simulation and the theoretical calculation by the speed triangle calculated method.

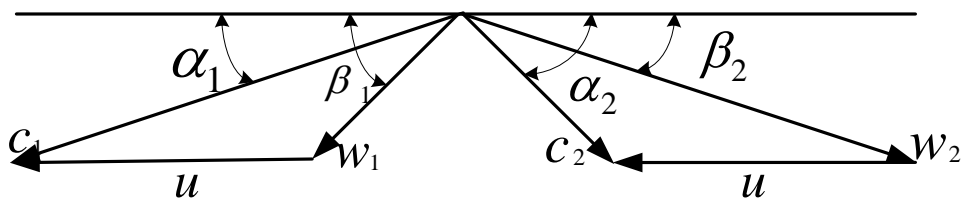


Fig.4 Speed triangle schematic diagram in rotor outlet

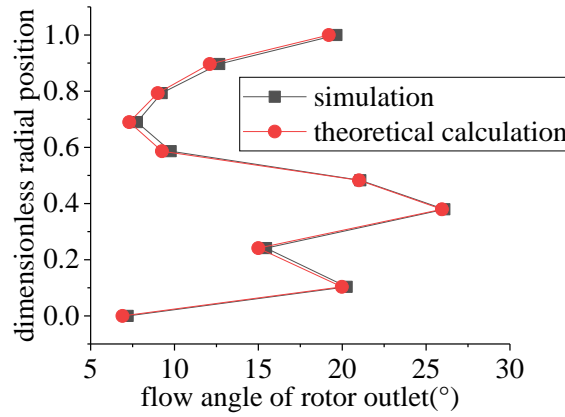


Fig.5 Comparison of rotor outlet flow angles between simulation and theoretical calculation

Under the rated back pressure 4.9 kPa condition, the steam flow angles at the outlet of rotor blade gradually decrease with the decrease of volume flow as shown in Fig.6(a). Under the 30% of the rated volume flow condition, the outlet angles of the rotor blade turn to negative at the 70% of the relative height of rotor blade. With the decrease of volume flow, the region of negative flow angles at the rotor blade outlet gradually increases. At 8% of the rated volume flow, the flow angles at the rotor blade outlet are negative value in 20%-85% of the relative height of rotor blade. The change rate of outlet flow angles is 7.31%. It is mainly because the steam flow is limited by the flow separation vortices. It can be seen in Fig.6(b) that when the back pressure rises to 15 kPa, at 70% of the rated volume flow, the flow angle at the outlet of the blade has a negative value at 70% of the relative height of rotor blade. The negative value reaches 50% of the relative blade height along the blade. With the decrease of volume flow, the negative outlet flow angles gradually develop toward tip and root direction. When the flow reduces to 8% of the rated volume flow, the negative outlet flow angles appear in the 88% to 2% of the relative blade height area. It indicates that a large volume of flow separation occurred in the rotor blade passage under this condition. The back pressure continues to rise to 30 kPa, at 100% of the rated volume flow, the outlet flow angles of rotor blade occur negative value at 70% of the relative height of rotor blade. When the flow decreases to 8% of rated volume flow, the change rate of outlet flow angles is 11.86%. The outlet flow angles under all volume flow conditions are seriously deviated from the design value as shown in Fig.6(d). The negative outlet flow angles occupy the whole blade height at 8% of the rated volume flow condition. It can be seen from Fig.6(a)~(d) that the decrease of the outlet angles of rotor blade is becoming smaller and smaller with the rise of the back pressure. The outlet flow angles of rotor blade have a tendency to decrease at the same volume flow conditions but the magnitude of the decrease is smaller than that at the same back pressure conditions. It is mainly because the flow field deterioration due to the decrease of volume flow is greater than that caused by back pressure changing. In addition, it can be seen from the figure that the outlet flow angles at the tip and root of rotor blade are chaotic, which is mainly due to the reflux caused by the tip clearance and the boundary layer.

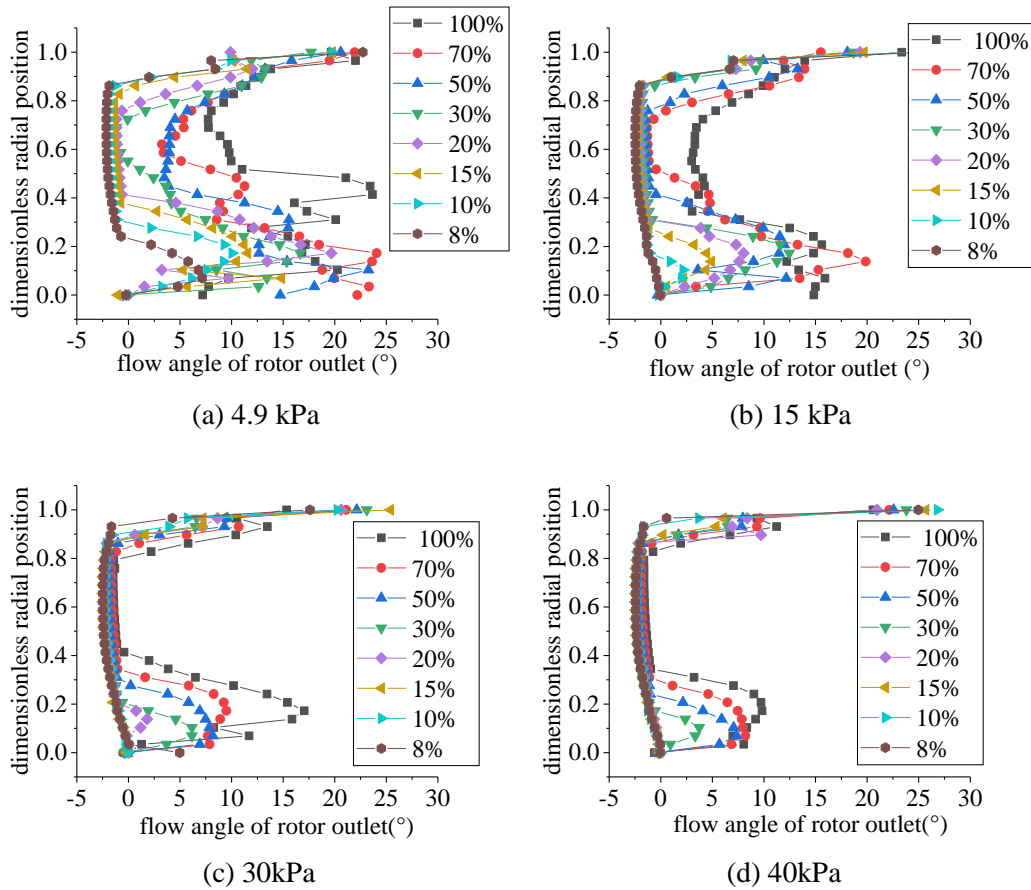
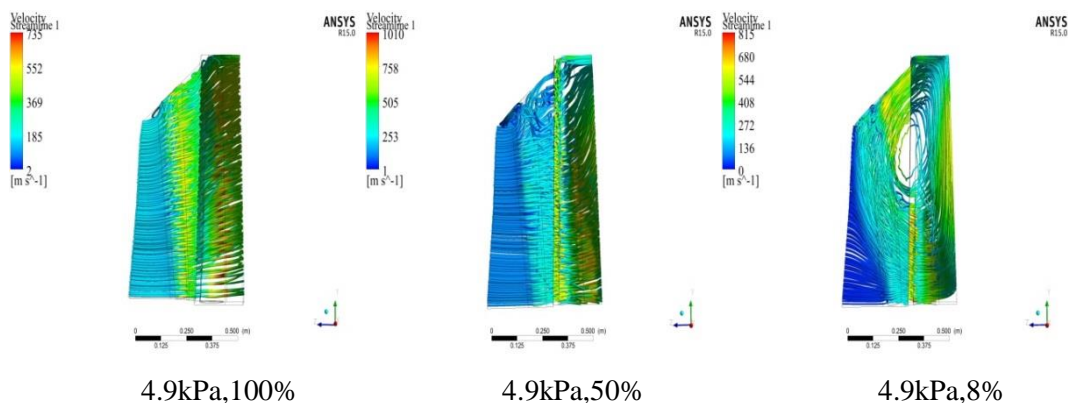


Fig.6. Flow angle of rotor outlet

The steam flow deflects when the volume flow reduces. The outlet flow angles gradually deviate from that under the rated condition and the negative attack angles occur, which are caused by the negative value of the flow angles at the outlet of the blade. With the increase of the negative attack angles, the range of flow separation is spreading. When the flow further decreases, the steam flows along the “diagonal” direction. The velocity triangle is severely deformed. In this case, a part of the energy must be consumed to counteract the reverse velocity for the steam to pass smoothly. It results in a decline in stage efficiency and becomes a serious threat to the safety of the blades.

### 3.2 Three dimensional streamline





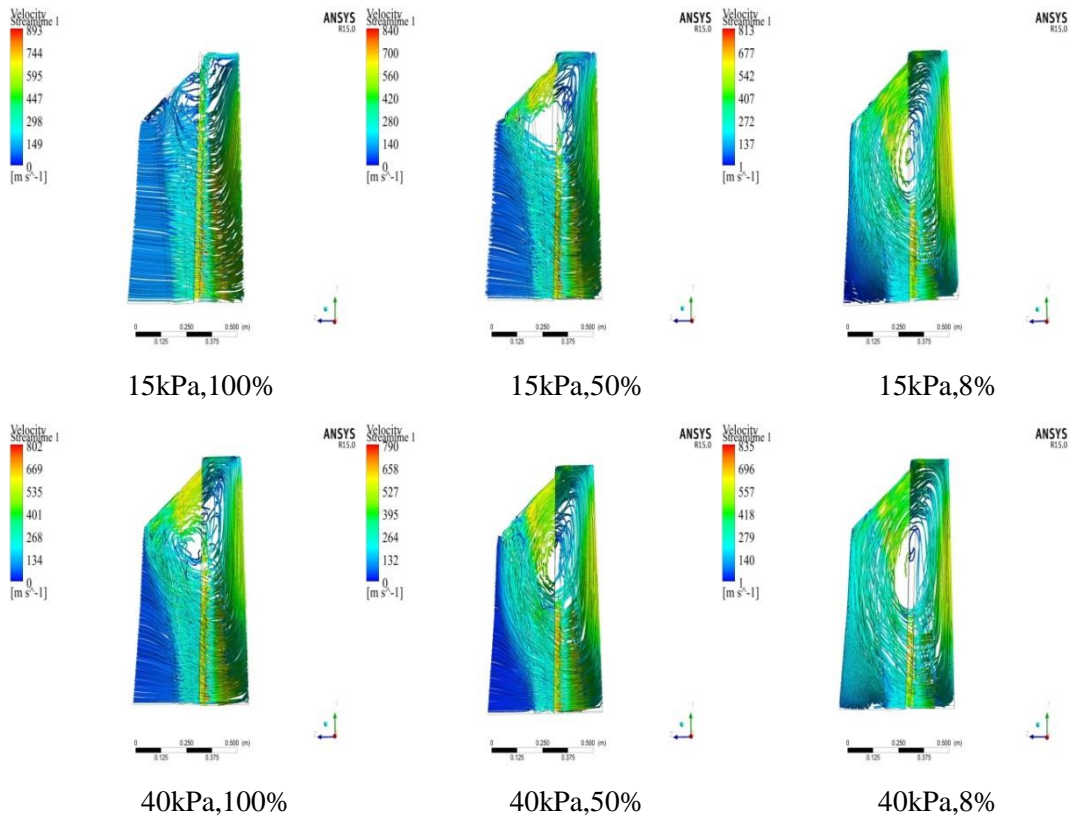


Fig.7. Three dimensional streamline of last stage blade

The three-dimensional streamlines of the last stage blade under different conditions are shown in Fig.7. It can be seen that the steam flows smoothly through the blade under the rated condition (4.9 kPa, 100% of the rated volume flow). With the volume flow decreases, the streamline curves. The streamline is squeezed toward the root in the stator blade but deflected to the tip of rotor blade. The streamline also curves and gradually forms vortices with the rise of back pressure. When the flow reduces to 50% of the rated volume flow, the streamline sharply curves but without vortex. When the flow further reduces to 8% of the rated volume flow, a vortex is formed in the gap between rotor and stator blade and a reverse region occurs at the root of rotor blade. Under the 15kPa back pressure, 100% of the rated volume flow condition, the streamline is severely curved but without vortex. At 50% of the rated volume flow condition, a vortex is formed between the rotor and stator blade and the vortex spreads along the blade with the decrease of volume flow. The back pressure rises to 40 kPa, the flow separation vortex is spread to 68% of the relative blade height. With the decrease of the volume flow, the radial flow of the steam becomes more and more typical and the influencing area of the flow separation vortex becomes larger. When the flow reduces to 8% of the rated volume flow, the vortex almost occupies the whole blade height and the steam flow can only fill the outer edge of the blade, which seriously affects the steam flow in the blade. At this point, the blades are completely in the so-called "blast" condition and no work is done.

### 3.3 Vortices cores position

Fig.8 shows the position of flow separation vortex cores in a small volume flow condition. It can be seen from the figure that under the same back pressure condition, the position of the vortex

cores moves to the root with the decrease of volume flow. Under the same volume flow condition, the position of the vortex cores decrease along the blade height with the rise of back pressure. It can be seen from the previous analysis, the vortex core starts to form at 4.9kPa back pressure and 30% of the rated volume flow condition and spreads to the root of rotor blade as the volume flow decreases. At 8% of the rated volume flow, the position of vortex core drops to 54.8% of the relative blade height. In addition, the influence of back pressure on the flow field is less than that of volume flow on the flow field. Therefore, under 15 kPa back pressure and 100% of the rated volume flow conditions, the streamline curves obviously but no vortex and vortex cores appear. When the back pressure rises to 30 kPa and the flow decreases to 20% of the rated volume flow, the vortex cores fluctuate slightly because of the interaction of flow separation and reverse vortices. As a result, the position of the flow separation vortex cores drops from 72.7% to 49.1% of the relative blade height.

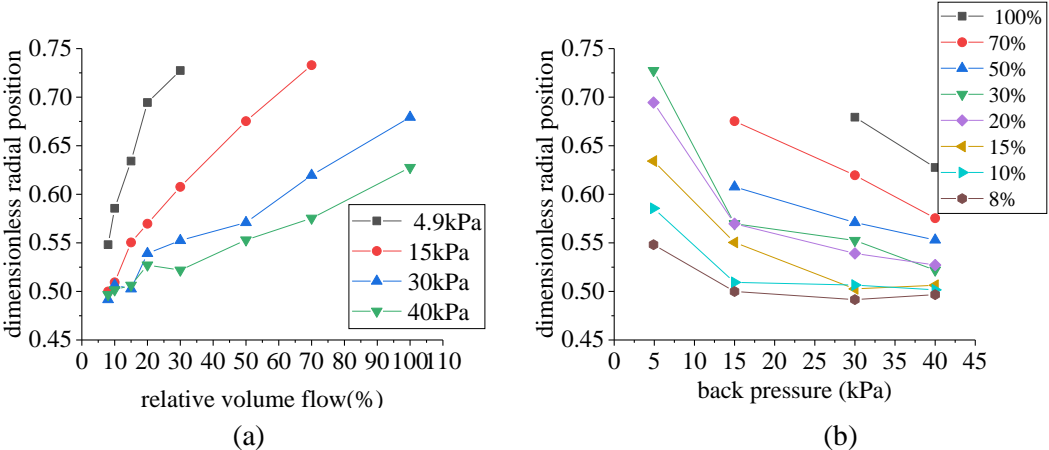


Fig.8 Flow separation vortex core position

**3.4 Influencing range of vortex cores**

Fig.9 displays the influencing range of vortex cores under different volume flow conditions when the back pressure are 4.9 kPa and 40 kPa. Maintaining the back pressure unchanged, the influencing range of the vortex cores will gradually enlarge in radial direction as the volume flow decreases. Under 40 kPa back pressure, 8% of the rated volume flow condition, the influencing range of vortex cores almost occupies the whole blade height. The position variation of the vortex cores under different volume flow conditions is the same with that the influencing range of vortex cores under the small volume flow conditions. With the decrease of volume flow, the influencing range of the vortex cores spreads not only in radial direction, but also in axial direction. If the volume flow continues to decrease, vortices may deteriorate the flow field at the last stages and cause the blade vibration, which will seriously threaten the safe operation of the blades.

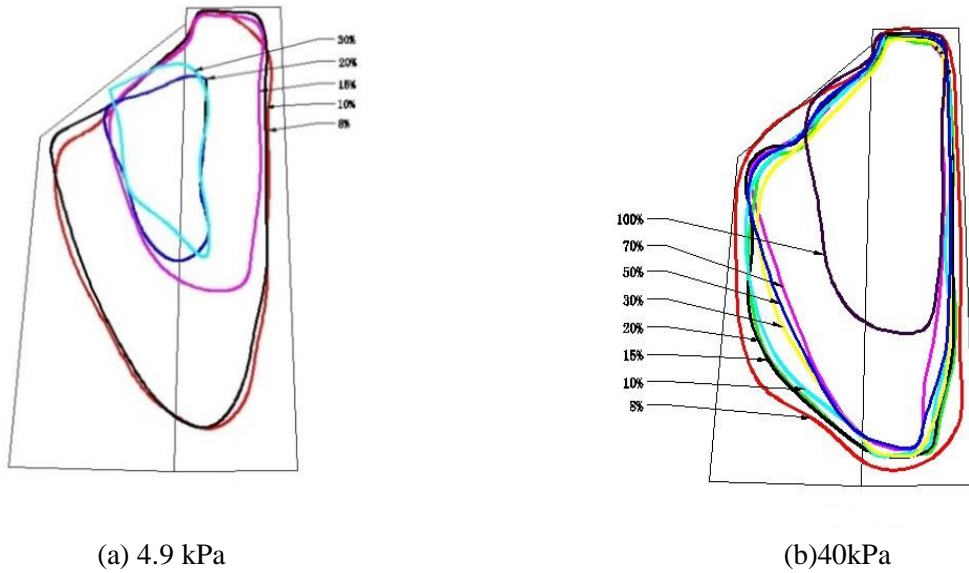


Fig.9 Influencing range of vortices cores

### 3.5 Limited streamline

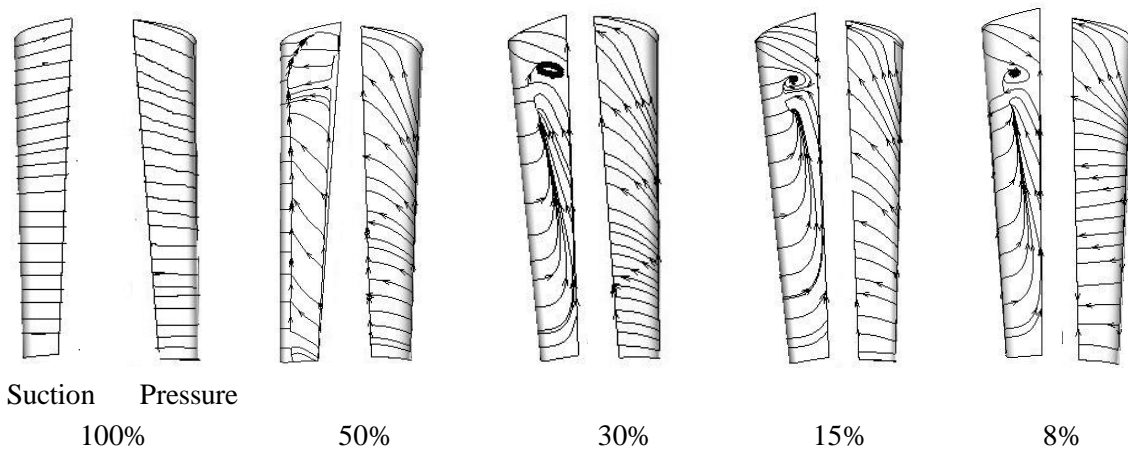


Fig.10 Limit streamline distribution of static blade

Fig.10 shows the distribution of the limit streamline of the stator under the rated back pressure and different volume flow conditions. As shown in the figure, under the rated condition, the steam flow on the suction and pressure surface of stator blade is relatively stable and the streamline passes through the stator blade smoothly. At 50% of the rated volume flow condition, the detached line and reattachment line appear on the suction surface. When the flow reduces to 30% of the rated volume flow, the steam flow of the suction surface is obviously deteriorated and the flow separation vortex first appears at the top of the blade. The separation area gradually spreads along the blade height with the volume flow further decrease. The streamline curves sharply and has a tendency to spread to the blunt under the influence of the flow separation vortices. The steam flow on the pressure surface is much better than that on the suction surface. The streamline curves slightly and no separation occurs at 50% of the rated volume flow. The curvature of streamline has no significant change with the decrease of volume flow. With the volume flow decreasing, the last stage blade is in a large negative attack angles condition and the flow separation occurs between rotor and stator. The separation flow

influences the performance of flow field of the last stage and causes the separation in suction of the stator blade. At the same time, the flow field deterioration does not influence the steam flow on pressure surface of stator blade under the rated back pressure condition, so the separation does not occur on the pressure surface of stator blade.

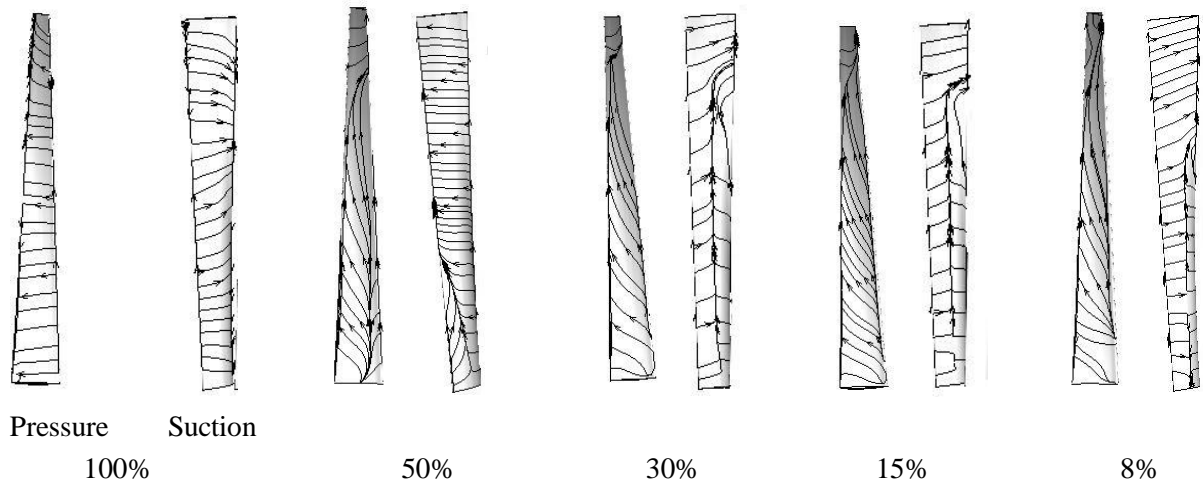


Fig.11 Limit streamline distribution of rotor blade

Fig.11 shows the distribution of the limit streamline of rotor blade under the rated back pressure and different volume flow conditions. It can be seen from the figure that the flow condition in the last stage rotor blade is good and the streamlines are distributed in the mainstream direction under the rated conditions. At 50% of rated volume flow conditions, a clear detached line and a reattachment line occur on the last rotor blade pressure surface. A vortex is formed on the suction surface of the last rotor blade in the reverse direction of the vortex on the pressure surface. When the flow reduces to 30% of the rated volume flow, the detached line and the reattached line of the pressure surface move to the blunt. The vortex at the suction surface merges into the vortex between the rotor and the stator. The vortex almost occupies the whole blade height under the condition of 8% of the rated volume flow, which seriously affects the safety of the last blade.

#### 4. Conclusion

(1) The outlet flow angles of the last stage blade begin to appear negative value and negative attack angles occur under the condition of rated back pressure and 30% of the rated volume flow. The range of negative attack angles becomes larger with the decrease of volume flow. When the volume flow further reduces, the steam flows along the “diagonal” direction. Part of the energy is consumed to counteract the reverse velocity for the flow of steam to pass smoothly, which threatens the safety of blades.

(2) A vortex first appears at the top clearance between the rotor and the stator at the rated back pressure and 30% of rated volume flow. The influencing range of vortex spreads to the root of blade with the decrease of volume flow. At 8% of rated volume flow conditions, the vortex almost occupies the whole blade height and interacts with the weak reverse vortex at the root of the blade. So the flow field of the last stage is affected seriously and the last stage blade is in the state of “blast”.

(3) The position of the flow separation vortex cores shifts from 72.7% to 49.1% of the relative

blade height with the decrease of volume flow. The influencing range of vortex cores extends in radial direction and has a tendency to spread to axial direction.

(4)The separation area is generated on the rotor pressure surface and gradually spreads to the suction surface with the decrease of volume flow. When the volume flow decreases to 30% of the rated volume flow, the steam flow on the suction surface in the last stator blade is affected by the separation area.

## Acknowledgement

This work was supported by National Key R&D Program of China (2017YFB0902100).

## Nomenclature

- $\alpha$  - wet steam dryness[-]  
 $h_{\text{sat, f}}(p)$  - saturated water enthalpy[J]  
 $h_{\text{sat, g}}(p)$  - saturated steam enthalpy[J]  
 $\varphi_{\text{mix}}(p)$  - wet steam thermophysical parameters[-]  
 $\varphi_{\text{sat, f}}(p)$  - saturated water thermophysical parameter[-]  
 $\varphi_{\text{sat, g}}(p)$  - saturated gas parameter[-]  
 $h_2$  - average enthalpy at the rotor outlet[J]  
 $h_2^{\text{is}}$  - average entropic enthalpy at the rotor outlet[J]  
 $h_1^*$  - average total enthalpy at the stator inlet[J]  
 $h_1^*$  - average enthalpy at the stator inlet[J]  
 $\beta_2$  - flow angle of rotor outlet[°]

## 5. References

- [1] L. Qi, Z.P. Zou, H.Z. Lu, Numerical Simulation of 3-Dimensional Flow in Last Two Stages of Air-cooled Steam Turbines, *Journal of Aerodynamics*, 2006, 01, pp. 144-149. (in Chinese)  
[2] Y.H. Xie, D. Zhang, Zh.P. Feng, A New Fatigue Model for Service Life Assessment of Last Stage Blade in Steam Turbine Based on Liquid Corrosion and Dynamic Stress, *Key Engineering Materials*, 2007, pp. 613-616.  
[3] T. Wollmann, N. Modler, M. Dannemann, Design and testing of composite compressor blades with focus on the vibration behaviour, *Composites Part A: Applied Science and Manufacturing*, 2017, 92, pp. 183-189.  
[4] H. Ma, F.T. Xie, H.Q. Nai, Vibration characteristics analysis of rotating shrouded blades with impacts, *Journal of Sound and Vibration*, 2006, 378, pp. 92-108.  
[5] R. Mandard, J.F. Witz, Y. Desplanques, Wavelet Analysis of Experimental Blade Vibrations During Interaction With an Abradable Coating, *Journal of Tribology*. 2014, 36, pp. 1-13.  
[6] N. Herzog, M. Binner, J.R. Seume, Verification of low-flow conditions in a multistage turbine, in: *ASME Turbo Expo 2007, Power for Land, Sea and Air*, 2007, pp. 183-190.  
[7] A. R. Rao, B.K. Dutta, Blade vibration triggered by low load and high back pressure, *Engineering Failure Analysis*. 2014, pp. 40-48.  
[8] J. D. Gill, V. R. Capece, R. B. Fost, Experimental methods applied in a study of stall flutter in an axial flow fan, *Shock and Vibration*, 2004, 11, pp. 597-613.  
[9] B. Adam, S. Havakechian, B. Megerle, On the Prediction and Theory of the Temperature Increase

- of Low Pressure Last Stage Moving Blades During Low Volume Flow Conditions and Limiting it Through Steam Extraction Methods, *Journal of Turbomachinery*. 2015, 137, 101002.
- [10]H. Joachim, S. Christian, Z. Frederik, Vortex-induced vibrations on a modern wind turbine blade, *Wind Energy*, 2016, 19, pp. 2041-2051.
- [11]L. Hoskoti, A. M. Mahesh, M. Sucheendran, Frequency lock-in during vortex induced vibration of a rotating blade, *Journal of Fluids and Structures*, 2018, 80, pp. 145-164.
- [12]X.CH. Zhu, H.T. W, D.W. Zhou, Numerical Study of Off-Design on LP Casing of Steam Turbine, *Thermal Turbine*, 2008, 01, pp. 51-53+70. (in Chinese)
- [13]X.S. Cai, F.X. Niu, T.B. Ning, Measurement of Flow and Wetness in Windage Condition in a 300 MW Direct Air-cooling Low Pressure Steam Turbine, *Proceedings of the CSEE*, 2009, 29, 2, pp. 1-7. (in Chinese)
- [14]H.L. Su, X.SH. Cai, Experimental Investigation into the Properties of Wet Steam Flow in Model Steam Turbine, *Proceedings of the CSEE*, 2004, 09, pp. 261-265. (in Chinese)
- [15] M. Benjamin, T.S. Rice, Numerical and Experimental Investigation of the Aerodynamic Excitation of a Model Low-Pressure Steam Turbine Stage Operating Under Low Volume Flow, *Journal of Engineering for Gas Turbines and Power*. 2012, 135, 012602.
- [16]R. Sigg, C. Heinz, M.V. Casey, Numerical and Experimental Investigation of a Low Pressure Steam Turbine During Windage, *Proc. Inst. Mech. Eng., Part A*, 2009, 223, pp. 697-708.
- [17] S. Naoki, F. Takao, I. Yoshifumi, An Experimental Investigation of the Influence of Flash-Back Flow on Last Three Stages of Low Pressure Steam Turbines, *Journal of Engineering for Gas Turbines & Power*, 2015, 137, pp. 1-10.
- [18]S. Naoki, F. Takao, I. Yoshifumi, An Experimental Investigation of the Influence of Flash-Back Flow on Last Three Stages of Low Pressure Steam Turbines, *Toshiba's selected papers on science & technology, Social infrastructure*, 2015, pp. 1-10.
- [19] S. Senoo, K. Segawa, H. Hamatake, Computations for Unsteady Compressible Flows in a Multistage Steam Turbine With Steam Properties at Low Load Operations, *ASME.J. Eng. Gas Turbines Power*. 2011, 133, 103001-103001-10.
- [20] I. Bosdas, M. Michel, K. Anestis, Unsteady Wet Steam Flow Field Measurements in the Last Stage of Low Pressure Steam Turbine, *Journal of Engineering for Gas Turbines & Power*, 2016, 138, pp. 1-12.
- [21]I. Bosdas, M. Mansour, I. Anestis, Unsteady Flow Field and Coarse Droplet Measurements in the Last Stage of a Low-Pressure Steam Turbine With Supersonic Airfoils Near the Blade Tip, *Journal of Engineering for Gas Turbines and Power*, 2017, 139, 091601.
- [22] K. Segawa, Steady and Unsteady Flow Measurements Under Low Load Conditions in a Low Pressure Model Steam Turbine, in: *International Conference on Nuclear Engineering and the ASME 2012 Power Conference*, 2012, pp. 833-839.
- [23]K.Zh. Huang, L. Cai, J.Sh. Gao, Numerical Investigation of Condensing Flow of Low Pressure Steam Turbine at Different Flow Rate Conditions, *Thermal Science*, 2017, pp. 161-167.